Journal for ImmunoTherapy of Cancer

C-reactive protein impairs immune response of CD8$^+$ T cells via FcγRIIb-p38MAPK-ROS axis in multiple myeloma

Jinxing Jiang ,[1] Ziyi Peng,[2] Junying Wang,[1] Mengping Chen,[1] Yike Wan,[1] Honghui Huang,[1] Zhiqiang Liu ,[2] Jingya Wang,[2] Jian Hou[1]

To cite: Jiang J, Peng Z, Wang J, *et al*. C-reactive protein impairs immune response of CD8$^+$ T cells via FcγRIIb-p38MAPK-ROS axis in multiple myeloma. *Journal for ImmunoTherapy of Cancer* 2023;**11**:e007593. doi:10.1136/jitc-2023-007593

► Additional supplemental material is published online only. To view, please visit the journal online (http://dx.doi.org/10.1136/jitc-2023-007593).

JJ, ZP and JuW contributed equally.

Accepted 15 September 2023

[1]Department of Hematology, Renji Hospital,Shanghai Jiao Tong University School of Medicine, Shanghai, China
[2]Department of Physiology and Pathophysiology, Tianjin Medical University, Tianjin, China

Correspondence to
Professor Jian Hou;
houjian@medmail.com.cn

Dr Jingya Wang;
jingyawang@tmu.edu.cn

ABSTRACT

Background C-reactive protein (CRP) is a prototypical acute phase protein in humans with the function of regulating immune cells. Serum CRP levels are elevated in multiple myeloma (MM), associated with MM cell proliferation and bone destruction. However, its direct effects on T lymphocytes in MM have not been elucidated.

Methods Public data sets were used to explore the correlation of CRP levels with immune cell infiltration and cytotoxicity score of CD8$^+$ T cells in MM. In vitro, repeated freeze-thaw myeloma cell lines were taken as tumor antigens to load dendritic cells (DCs) derived from HLA-A*0201-positive healthy donors. MM-specific cytotoxic T cells (MM-CTL) were obtained from T lymphocytes of the corresponding donors pulsed with these DCs. B-cell maturation antigen (BCMA)-targeted chimeric antigen receptor (CAR)-T cells were manipulated by transfecting with lentivirus encoding an anti-BCMA single-chain variable fragment. Then T cells from healthy controls, MM-CTLs and BCMA CAR-T cells were exposed to CRP and analyzed for cell proliferation, cytotoxicity, immunophenotypes. CRP binding capacity to T cells before and after Fc gamma receptors IIb (FcγRIIb) blockage, p38 mitogen-activated protein kinase (MAPK) pathway and the downstream molecules were also detected. In vivo, both normal C57BL/6J mice and the Vk*MYC myeloma mouse models were applied to confirm the impact of CRP on T cells.

Results CRP levels were negatively correlated with cell-infiltration and cytotoxicity score of CD8$^+$ T cells in MM. In vitro experiments showed that CRP inhibited T-cell proliferation in a dose-dependent manner, impaired the cytotoxic activity and upregulated expression of senescent markers in CD8$^+$ T cells. In vivo results validated the suppressive role of CRP in CD8$^+$ T cells. CRP could bind to CD8$^+$ T cells, mainly to the naïve T subset, while the binding was dramatically decreased by FcγRIIb blockage. Furthermore, CRP resulted in increased phosphorylation of p38 MAPK, elevated levels of reactive oxygen species and oxidized glutathione in CD8$^+$ T cells.

Conclusions We found that CRP impaired immune response of CD8$^+$ T cells via FcγRIIb-p38MAPK-ROS signaling pathway. The study casted new insights into the role of CRP in anti-myeloma immunity, providing implications for future immunotherapy in MM.

WHAT IS ALREADY KNOWN ON THIS TOPIC

⇒ C-reactive protein (CRP) binds to immune cells including B cells, dendritic cells via Fc gamma receptors and exerts immunomodulatory effects in adaptive immunity.

⇒ CRP promotes multiple myeloma (MM) cell proliferation and bone destruction and is associated with poor outcomes in patients with MM. However, its direct effects on T lymphocytes in MM have not been elucidated.

WHAT THIS STUDY ADDS

⇒ We found that CRP could bind to CD8$^+$ T cells and impaired immune response of CD8$^+$ T cells via FcγRIIb-p38MAPK-ROS signaling pathway.

HOW THIS STUDY MIGHT AFFECT RESEARCH, PRACTICE OR POLICY

⇒ The Fc gamma receptors IIb (FcγRIIb) blocking antibody or p38 mitogen-activated protein kinase (MAPK) inhibitor might rescue CD8$^+$ T cells from the inhibition of CRP. The study provides implications for future immunotherapy in MM with high CRP levels.

BACKGROUND

C-reactive protein (CRP) is a highly conserved protein of the pentraxin family with five identical subunits.[1] It maintains at low levels in normal condition, but can reach upwards to 500 mg/L in response to an acute-phase stimulus.[2] Inflammatory cytokines such as interleukin (IL)-1 and IL-6 act as intermediaries that induce plasma CRP production by hepatocytes in the liver. CRP is known to be involved in innate immunity through opsonization and phagocytosis by binding to surface-exposed phosphatidylserine, complement component C1q[3] and Fc gamma receptors (FcγRs).[4]

In recent years, the role of CRP in adaptive immunity has attracted increasing attention. In systemic lupus erythematosus, CRP suppresses autoimmune responses including

clearing apoptotic cells and autoantigens by activating complement and FcγRs.[5] In autoimmune encephalomyelitis, CRP reduces the number of dendritic cells (DCs), as well as inhibits maturation of DCs through Fc gamma receptors IIb (FcγRIIb, CD32b), leading to immune tolerance of peripheral T cells.[6 7] Moreover, CRP-treated DCs activate T cells and induce Th1 cell responses, promoting atherosclerotic progression.[8] Collectively, CRP has been reported to regulate T lymphocytes indirectly through DCs. According to researches about the role of CRP in directly regulating T cells, CRP binds specifically to human Jurkat T cells and to mouse naive $CD4^+$ T cells, then modulates the Th1 and Th2 responses.[9] In addition, CRP inhibited the early stage of T-cell receptor engagement and suppressed the formation of immune synapses, eventually resulting in inhibition of T-cell proliferation in patients with melanoma.[10] However, the receptors on T cells for CRP remain obscured, the downstream molecular mechanisms warrant further investigation as well.

Accumulating evidences have strongly suggested that high CRP levels are present and associated with poor outcomes in patients with multiple myeloma (MM),[11 12] melanoma,[13] breast cancer.[14] Elevated CRP in patients with MM promotes MM cell proliferation and bone destruction. As a result, CRP has been recognized as an indicator to evaluate the progression of MM.[15] Mechanistic studies revealed that CRP binds to FcγRII on the surface of MM cells, activates PI3K/Akt, ERK, and NF-κB pathways to promote MM cell proliferation and protect MM cells from chemotherapy-induced apoptosis.[11] CRP also activates p38 mitogen-activated protein kinase (MAPK) - TWIST pathway on binding to FcγRII on myeloma cells and stimulates osteolytic cytokine secretion.[16] As of yet, there has been no report about the direct regulation of CRP in T lymphocytes in anti-myeloma immunity.

Despite significant improvement in the treatment of MM, the disease remains incurable. The development of T-cell redirecting therapies, such as chimeric antigen receptor (CAR) T cells targeted B-cell maturation antigen (BCMA), have transformed the outcome of triple-class exposed relapsed and refractory MM (RRMM).[17]Generally, RRMM are accompanied by high CRP levels. Therefore, we sought to determine whether CRP interfered with CAR-T cell function. During the anti-MM immune response, MM antigen-specific cytotoxic T cells (MM-CTL) exhibit specific cytotoxic activity directly against MM cells. Collectively, T cells from healthy controls, MM-CTLs and BCMA CAR-T cells were chosen to study the direct effects of CRP on T lymphocytes.

MATERIALS AND METHODS

Patient samples and T-cell culture

Peripheral blood samples were obtained from healthy volunteers under an Institutional Review Board-approved protocol. Age-matched healthy controls were recruited following the exclusion criteria: any type of tumors, inflammatory or autoimmune diseases, active infection. Peripheral blood mononuclear cells (PBMCs) were isolated by density gradient with Ficoll-Paque (GE Healthcare, USA). For cryopreservation, PBMCs were re-suspended in CELLSAVING (New Cell & Molecular Biotech, China), frozen at −80°C and stored in liquid nitrogen. $CD8^+$ T cells were isolated using a magnetic negative selection kit (Miltenyi Biotec, Germany) and cultured in T-cell culture medium (STEMCELL Technologies, Canada). PBMCs or purified $CD8^+$ T cells were stimulated using CD3/CD28 coated dynabeads (Invitrogen, USA) at a ratio of 1:1 with 300 IU/mL IL-2 (PeproTech, USA) for 2 days, and then magnetic beads were removed and CRP was added into the T-cell media.

Apoptosis and cell-proliferation assays

Apoptosis of T cells was determined using flow cytometry with Annexin V Apoptosis detection kit (Beyotime, China). Proliferation of T cells was measured using cell counting, CFSE analysis and Ki67 detection.

Flow cytometry analysis

For surface marker staining, PBMCs treated with CRP for 5 days were obtained. About 2×10^5 cells were re-suspended in phosphate-buffered saline (PBS) containing 2% fetal bovine serum (FBS) and stained with the antibody cocktail for 30 min at room temperature in the dark. For intracellular cytokine staining, cells were stained for intracellular cytokines after fixation and permeabilization followed by cell surface marker staining. All samples were acquired with a DxFlex system (Beckman Coulter) and analyzed using FlowJo software (V.10.5.3). Antibodies used for cell surface staining or intracellular staining were listed in online supplemental table S1.

Senescence-associated β-galactosidase assay

Purified $CD8^+$ T cells were treated with CRP (50 µg/mL) after activation of CD3/CD28 beads, as described above. After incubation for 5 days, $CD8^+$ T cells were collected for senescence-associated β-galactosidase (SA-β-Gal) staining according to the manufacturer's instructions.

Western blotting

After treatment of CRP for 5 days, $CD8^+$ T cell total protein was extracted using RIPA buffer (Beyotime, China) with protease inhibitor and phosphatase inhibitor (Beyotime, China). Total cellular protein was mixed with a 5X loading buffer (Beyotime, China) to a final concentration of 1X sample buffer and then heated at 100°C for 10 min. Protein was loaded onto 10% SDS PAGE gels, incubated with the primary and secondary antibodies after protein transfer, and imaged using Immobilon Western Chemiluminescent HRP Substrate (Merck, USA). The results were analyzed using the ImageJ Software. The antibodies used in the western blot protein analysis are listed in online supplemental table S2.

CRP binding

CRP was incubated with T cells from healthy controls for 30 min at 4°C in PAB buffer (PBS, 0.1% BSA, 0.05%

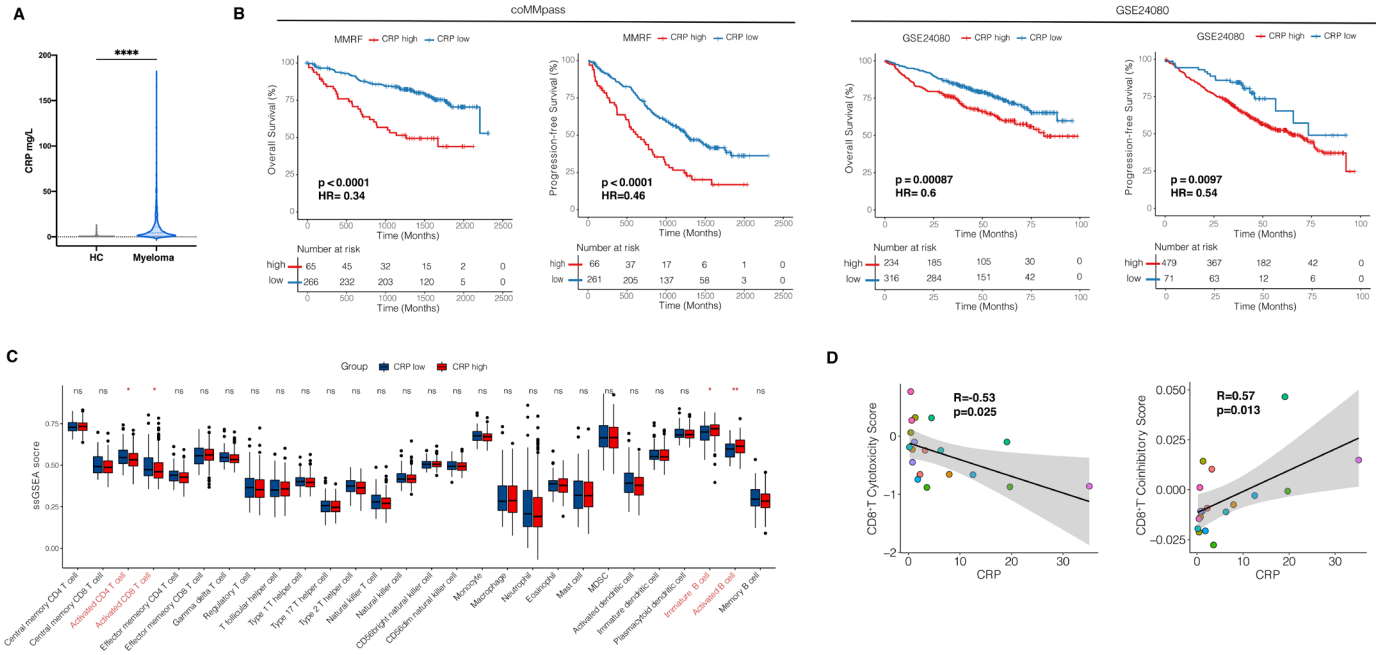

Figure 1 CRP levels are correlated with functional status of T cells in MM. (A) Patients with MM had elevated CRP concentrations compared with healthy controls. (B) The Kaplan-Meier survival curves showed that high CRP levels predicted poor OS time and EFS time in MM samples from MMRF coMMpass and GSE24080 (log-rank test). (C) The differential scores of 28 immune cell type signatures by ssGSEA method in patients from CoMMpass database with low and high CRP levels. (D) Scatterplots showing Pearson correlations between CRP levels with scores of cytotoxicity and coinhibitory per patient in our single-cell RNA data set. Statistical analysis performed by Wilcoxon test. CRP, C-reactive protein; HC, healthy controls; MM, multiple myeloma; OS, overall survival.

NaN3, 1 mM Ca). After washing twice with PAB, cells were incubated sequentially with anti-CRP mAb or IgG FITC-Isotype control, then flow cytometry was conducted for analysis. Activated T cells were treated with anti-CD32b (5 µg/10^6 cells) for 1 hour 4°C in PBS buffer, after washing twice, CRP binding was detected for blocking of CD32b analysis.

Total cellular ROS measurement

For analysis of total cellular reactive oxygen species (ROS), $CD8^+$ T cells were incubated with 5 mM DCFDA (2',7'-dichlorofluorescein diacetate, Nanjing Jiancheng, China) at 37°C for 30 min. Cells were washed twice with cold PBS and immediately analyzed with flow cytometry. All samples were acquired with a DxFlex system (Beckman Coulter) and analyzed using FlowJo software (V.10.5.3).

Glutathione detection assay

The levels of intracellular glutathione in $CD8^+$ T cells were determined using the reduced glutathione (GSH) assay kit and total glutathione/oxidized glutathione assay kit (Nanjing Jiancheng, China) according to the manufacturer's instructions.

MM cell culture

MM cell lines including RPMI-8226, OPM2, U266 were preserved in Renji Hospital. MM cell lines were cultured in RPMI-1640 (Thermo, USA) supplemented with 10% FBS, 100 IU/mL penicillin and 100 µg/mL streptomycin. All cell lines were maintained at 37°C in an incubator with 5% CO_2.

BCMA CAR-T cells transduction and cytotoxicity assay

T cells were purified from PBMCs using microbeads (Miltenyi Biotec, Germany) and were stimulated with anti-CD3 and anti-CD28 monoclonal antibodies. Stimulated T cells were transduced with the lentiviral vector encoded as an anti-BCMA single-chain variable fragment linked to CD28, OX40, and CD3ζ signaling domains as previously reported.[18]

CRP was added on day 3–5 of transduction and maintained for 5 days. For target-specific assay, target cells RPMI-8226 were incubated with CFSE at 5 µM for 20 min at 37°C, and then washed with complete medium. Then BCMA CAR-T cells were cocultured with RPMI-8226 at an effector: target ratio of 1:1, 5:1, 10:1, 20:1 and 40:1 for 6 hours. After the incubation, following a further wash, cells were labeled for 15 min with PI (Absin, China) to identify dead cells and then detected by flow cytometry. The $CFSE^+PI^-$ cells were alive target cells and the $CFSE^+PI^+$ cells were dead target cells. Spontaneous dead targets were obtained from targets incubated with medium alone.

Generation of myeloma specific T cells

PBMCs from HLA-A*0201-positive healthy donors were cultured in the incubator for 2 hours to allow cell attachment to culture dish. Cells not adherent to culture dish

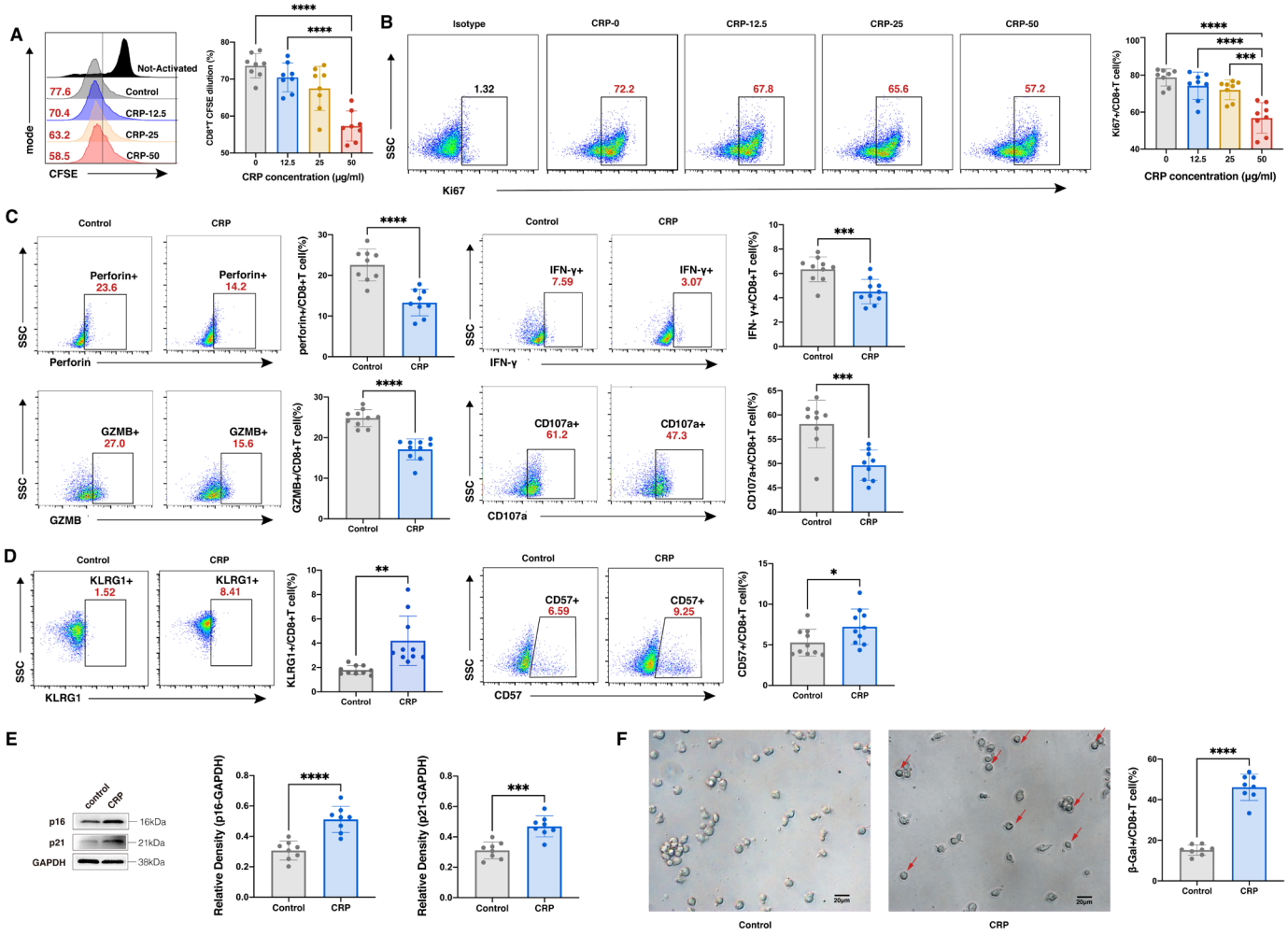

Figure 2 CRP inhibits the proliferation and cytotoxicity, also induces senescent phenotype of CD8$^+$ T cells. PBMCs were activated with CD3/CD28 beads in the presence of CRP at doses of 0, 12.5, 25 or 50 µg/mL for 5 days. (A) Proliferation analysis of Cell Trace CFSE-labeled CD8$^+$ T cells treated with different concentration of CRP. The dilution of CFSE$^+$ CD8$^+$ T cells was detected. (B) CD8$^+$ T cells treated with different concentration of CRP were stained with antibody against Ki67 to detect the proliferation by flow cytometry. A representative flow-cytometry plot of Ki-67 staining in CD8+T cells was shown. (C) The perforin$^+$, GZMB$^+$, IFN-γ$^+$ and CD107a$^+$ T cells proportions (gated on CD8$^+$ T cell) were examined by flow cytometry. Representative data were from one of eight patients. (D) The expression of KLRG1 and CD57 in CD8$^+$ T cells treated with CRP were detected. (E) Purified CD8$^+$ T cells were treated with CRP (50 µg/mL) for 5 days, and then subjected to western blot for assessment of p16 and p21. (F) Purified CD8$^+$ T cells were stained for SA-β-Gal activity and statistical analysis was performed. SA-β-Gal positive cells are indicated by red arrows. Data from eight independent experiments are shown. *p<0.05, **p<0.01, ***p<0.001. CRP, C-reactive protein; GZMB, granzyme B; IFN, interferon; PBMCs, peripheral blood mononuclear cells; SA-β-Gal, senescence-associated β-galactosidase.

(majorly T cells) were collected and frozen in liquid nitrogen for subsequent experiments. The adherent cells (CD14$^+$ monocytes) were exposed to 1000 U/mL GM-CSF (PeproTech, USA) plus 1000 U/mL IL-4 (PeproTech, USA) for 5 days, and then with 50 ng/mL TNF-α (PeproTech, USA) for one additional day. On day 6, DCs were cultured with lysate of tumor cells (50 µg/mL) prepared by freeze-then-thaw method. Mature DCs were harvested and cocultured with T cells after thawing for three cycles.

In vivo experiments

C57BL/6J mice (6–8 weeks of age, both sexes) received intravenous injection of murine myeloma Vk*MYC cells (1×10^6 cells per mouse) and 3 weeks later, both Vk*MYC mice and C57BL/6J mice received intravenous injection of CRP (50 µg/mouse) or PBS, respectively, to investigate the impact of CRP on T cells in vivo. We also compared the expression of CD32b on T cells from normal C57BL/6J mice and Vk*MYC myeloma mice without CRP injection. Two days later, mononuclear cells from the spleen and bone marrow were collected and flow cytometry was conducted.

Quantification and statistical analysis

Data are represented as mean±SEM, and analyzed using analysis of variance with the Bonferroni correction. For experiments involving only two groups, Student's t-test was used. Kaplan-Meier was used to analyze clinical

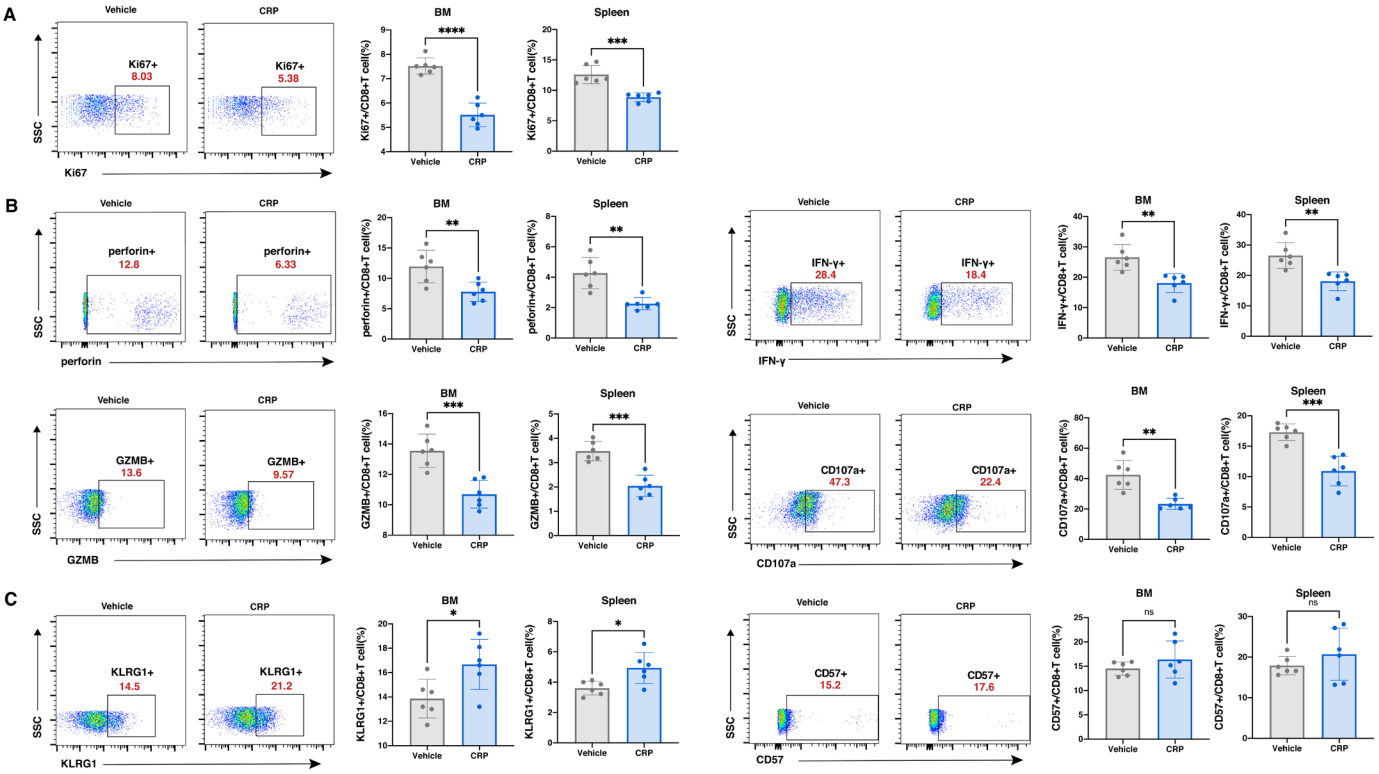

Figure 3 CRP impairs CD8$^+$ T cells function in murine models. CD8$^+$ T cells from BM and spleen in C57BL/6 mice after CRP intervention. (A) Proliferation analysis of CD8$^+$ T cells treated with CRP using anti-Ki67 antibody. (B–C) The perforin$^+$, GZMB$^+$, IFN-γ$^+$ and CD107a$^+$ T cells proportions (B) as well as the expression of KLRG1 and CD57 (C) were examined by flow cytometry. Data from six independent experiments are shown. *p<0.05 **p<0.01 ***p<0.001. BM, bone marrow; CRP, GZMB, granzyme B; IFN, interferon.

prognosis and Pearson's correlation was used to analyze correlation, p<0.05 was considered statistically significant.

RESULTS

CRP level are correlated with functional status of T cells in MM

Serum CRP concentration was significantly higher in patients with MM compared with healthy donors (figure 1A, p<0.0001). Patients with low CRP concentration had longer overall survival (OS) as well as progression-free survival (PFS) in patients with MM from the MMRF CoMMpass (https://research.themmrf.org) and GSE24080 data set[19] (p<0.01 for both OS and PFS; figure 1B). The ssGSEA analysis of the MMRF CoMMpass cohort showed lower infiltration of activated CD4$^+$ and CD8$^+$ T cells in patients with MM with high serum CRP (figure 1C). Furthermore, in our single-cell sequencing data,[20 21] elevated serum CRP in patients with MM correlated with lower cytotoxicity score and higher inhibitory score in CD8$^+$ T cells (figure 1D). Analysis of clustering was shown in online supplemental figure S1A,B.

CRP inhibits the proliferation and cytotoxicity, also induces senescent phenotype of CD8$^+$ T cells

In cultured CD3/CD28-activated T cells, CRP exposure (0–50 µg/mL) inhibited the proliferation of both CD8$^+$ T cells and CD4$^+$ T cells through cell counting in a concentration-dependent and time-dependent manner (online supplemental figure S2A,B). To identify CD8$^+$ and CD4$^+$ T cells via flow cytometry, the gating strategy was shown in online supplemental figure S2C. Relative to control-treated cells, CRP exposure at 50 µg/mL for 5 days produced 17.94% inhibition of proliferation with CD8$^+$ T cells, and 13.83% inhibition of CD4$^+$ T cells. CRP intervention also decreased the frequencies of CFSE^{low} CD8$^+$ T cells and Ki67$^+$ CD8$^+$ T cells in a concentration-dependent manner (figure 2A,B). Similarly, the CFSE^{low} CD4$^+$ T cells and Ki67$^+$ CD4$^+$ T cells were also declined after CRP exposure (online supplemental figure S2D,E). Compared with cells without CRP treatment, CRP exposure at 50 µg/mL for 5 days decreased 22.16% of CFSE^{low} CD8$^+$ T cells and 23.92% of Ki67$^+$ CD8$^+$ T cells, as well as 16.93% of CFSE^{low} CD4$^+$ T cells and 17.05% of Ki67$^+$ CD4$^+$ T cells. Collectively, CRP inhibited proliferation of T cells, especially CD8$^+$ T cells. However, CRP incubation did not alter the apoptosis of CD8$^+$ T cells (online supplemental figure S2F).

To determine whether CRP altered T-cell phenotypes, CD8$^+$ T cells were categorized based on CD45RA and CCR7 expression into naïve T (CD45RA$^+$CCR7$^+$), central memory T (CD45RA$^-$CCR7$^+$), effector memory T (CD45RA$^-$ CCR7$^-$) and effector T (CD45RA$^+$CCR7$^-$) populations. CRP treatment reduced the frequency of naïve T in CD8$^+$ T cells (online supplemental figure S2G). In CD4$^+$ T-cell subsets, there were no significant changes

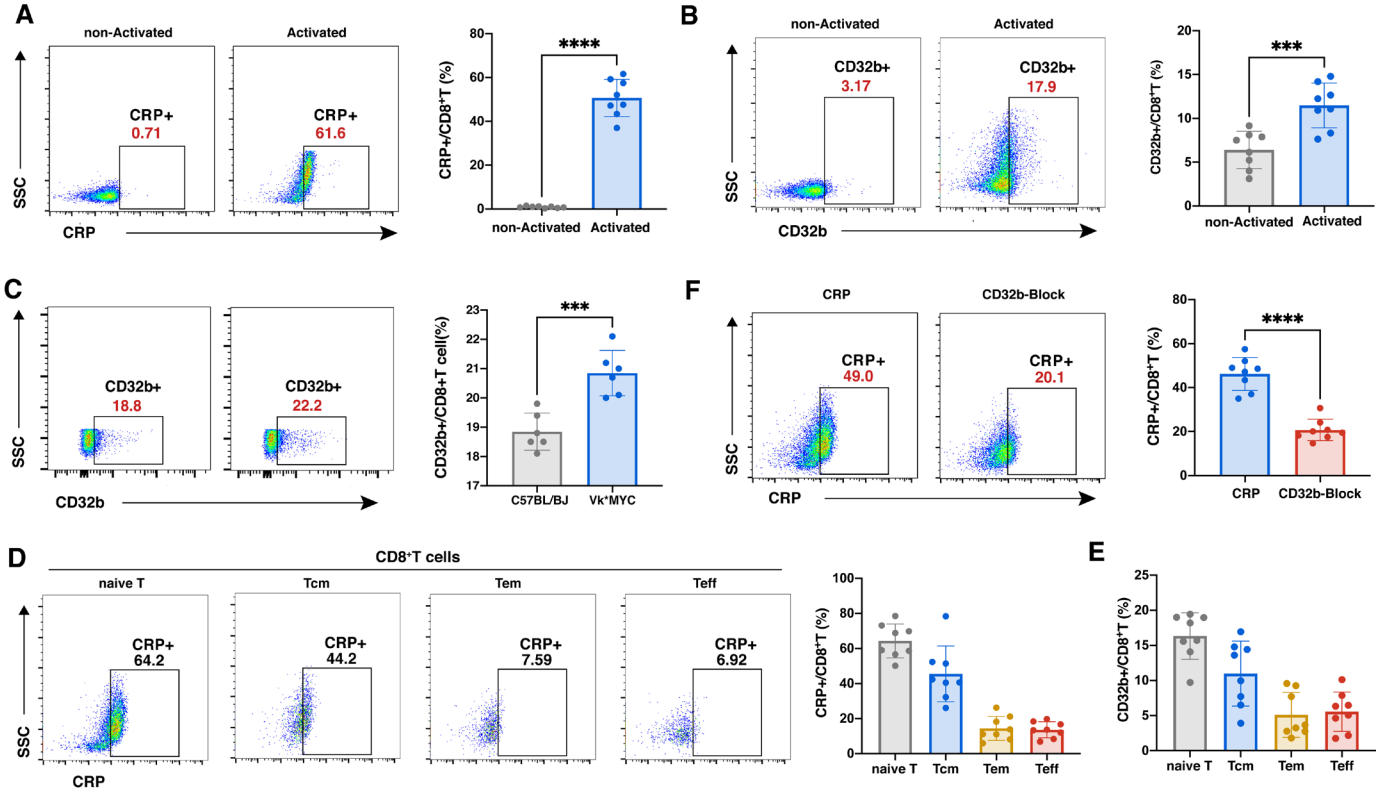

Figure 4 CRP binds FcγRIIb on activated CD8$^+$ T cells. (A) The frequency of CRP-treated CD8$^+$ T cells from healthy controls before or after activation is stained with anti-CRP antibody by flow cytometry. (B) The expression of CD32b for CD8$^+$ T-cell populations before or after activation. (C) The frequencies of CD32b$^+$ cells in CD8$^+$ populations from BM in C57BL/6 and Vk*MYC mice. Data from six independent experiments are shown. (D) Frequency of CRP$^+$ cells in different subsets of CD8$^+$ T cells. (E) The proportion of CD32b$^+$ cells in CD8$^+$ T-cell compartments. (F) Flow cytometry assay showing the binding ratios of CRP to CD8$^+$ T cells obtained from healthy individuals with treatment of PBS (left) or anti-CD32b (right). Each symbol represents an individual subject. Data from eight independent experiments are shown. **p<0.01, ***p<0.001, ****p<0.0001. BM, bone marrow; CRP, C-reactive protein; FcγRIIb, Fc gamma receptors IIb; PBS, phosphate-buffered saline; Tcm, central memory T; Teff, effector T; Tem, effector memory T.

in subpopulation of regulatory T cells (Treg) (CD127^{low}CD25^{high}), Th1 (CD183$^+$CD196$^-$), Th2 (CD183$^-$CD196$^-$) or Th17 (CD183$^-$CD196$^+$) after CRP intervention (online supplemental figure S2H).

Decreased expression of perforin, granzyme B (GZMB), interferon (IFN)-γ and CD107a and increased expression of KLRG1 and CD57 were present in activated CD8$^+$ T cells with CRP treatment (figure 2C,D). The protein levels of p16 and p21, as well as the activity of SA-β-Gal in CD8$^+$ T cells were also elevated after CRP exposure (figure 2E,F). We then evaluated expression of exhaustion markers on T cells after CRP treatment. There were no changes in the expression of TIGIT, TIM3, PD1, CTLA4 but increased expression of LAG3 on CD8$^+$ T cells with CRP intervention (online supplemental figure S2I). Taken together, CD8$^+$ T cells with treatment of CRP held impaired proliferation, decreased cytotoxicity and senescence phenotype.

CRP impairs CD8$^+$ T cells function in murine models

The inhibition impact of CRP on T cells was also observed in C57BL/6J mice. CD8$^+$ T cells from bone marrow (BM) and spleen in mice receiving CRP both exhibited declined Ki67 expression (figure 3A, p<0.05) and decreased levels of perforin, GZMB, IFN-γ and CD107a (figure 3B). CRP also upregulated the expression of KLRG1 as well as LAG3, without significant changes in the expression of CD57 or PD1 (online supplemental figure S3A,B).

CRP binds to FcγRIIb on activated CD8$^+$ T cells

T cells which did not stimulate with CD3/CD28 beads displayed none-CRP bound on the surface, while about 47% of CD8$^+$ T cells and 37% of CD4$^+$ T cells were positive for CRP after activation with the incubation of CRP (figure 4A, online supplemental figure S4A). As FcγRs were identified as receptors for CRP, we further queried the expression of different FcγR on T cells and found that FcγRI (CD64), FcγRIIA (CD32a), FcγRIIc (CD32c), FcγRIII (CD16) were barely expressed on T cells while FcγRIIb$^+$ T cells were about 6.29% (online supplemental figure S4B). Furthermore, the frequency of FcγRIIb$^+$ T cell was significantly increased in CD8$^+$ T cells after activation (figure 4B), as well as in CD4$^+$ T cells (online supplemental figure S4E), but there were no changes in the expression of FcγRI, FcγRIIA, FcγRIIc and FcγRIII (CD16) after T-cell activation (online supplemental figure S4C). Diagram of CD32b gating strategy was shown

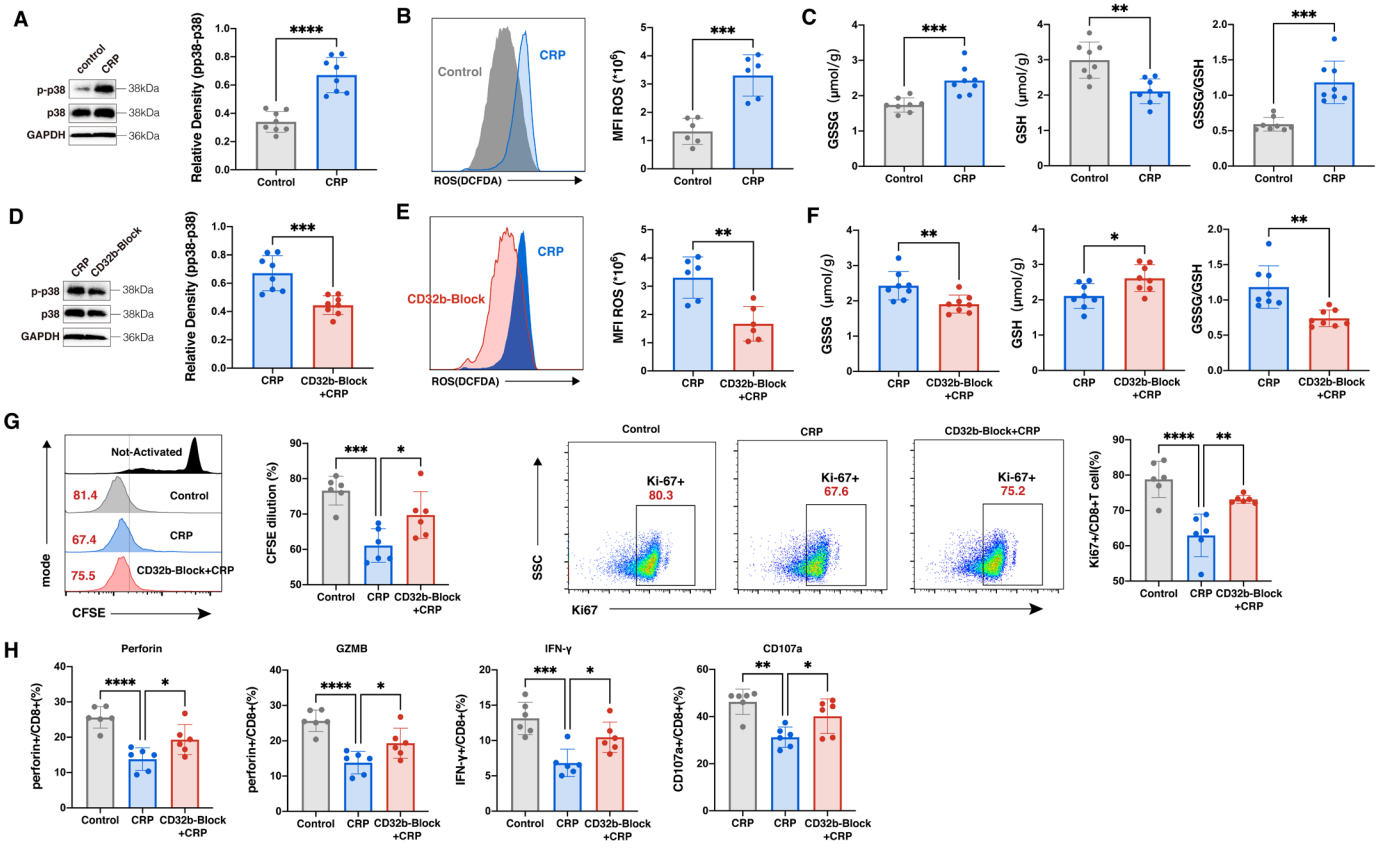

Figure 5 CRP regulates p38MAPK/ROS in a CD32b-dependent manner. (A) Purified CD8$^+$ T cells were treated with CRP (50 µg/mL) for 5 days, and then subjected to western blot for assessment of p38 MAPK signaling pathway. (B) FACS-based quantification of total cellular ROS in purified CD8$^+$ T cells in the presence of CRP for 5 days. (C) Microplate label-based quantification of oxidized glutathione and reduced glutathione in CD8$^+$ T cells treated with CRP. (D) CD8$^+$ T cells treated with CD32b blockage before CRP (50 µg/mL) treatment and then p38 MAPK pathway was detected. (E) Assessment of total cellular ROS in purified CD8$^+$ T cells in the with CD32b blockage. (F) Quantification of oxidized glutathione and reduced glutathione in CD8$^+$ T cells with blockage of CD32b. (G) CRP-treated CD8$^+$ T cells with CD32b blockage were stained with CFSE and Ki67 to detect the proliferation by flow cytometry. (H) The perforin$^+$, GZMB$^+$, IFN-γ$^+$ and CD107a$^+$ T cells proportions (gated on CD8$^+$ T cell) were examined by flow cytometry. Data from eight independent experiments are shown. *p<0.05, p<0.01, ***p<0.001, ****p<0.0001. CRP, C-reactive protein; DCFDA, 2',7'-dichlorofluorescein diacetate; GSH, glutathione; GSSG, oxidized glutathione; GZMB, granzyme B; IFN, interferon; MAPK, mitogen-activated protein kinase, ROS, reactive oxygen species.

in online supplemental figure S4D. In vivo, the expression of CD32b was increased in CD8$^+$ T cells separated from BM in Vk*MYC mice compared with normal C57BL/6J mice without CRP injection (figure 4C). Among different subsets in CD8$^+$ T cells, naïve T was the major contributor to bind CRP (figure 4D). We further examined the expression of CD32b and found the naïve CD8$^+$ T cell subset contained the highest frequencies of CD32b$^+$ cells (figure 4E). Given the expression of CD32b on T cells, we considered its role in the binding of CRP to T cells. Pretreatment of CD8$^+$ T cells and CD4$^+$ T cells from healthy individuals with anti-CD32b antibodies caused a significant decline in the binding rate of CRP (figure 4F, online supplemental figure S4F). These data supported the CRP bound to FcγRIIb on the surface of CD8$^+$ T cells, especially the naïve T subset.

CRP regulates p38MAPK/ROS in a CD32b-dependent manner

Treatment with CRP increased the protein levels of phosphorylated p38 (pp38) in CD8$^+$ T cells from healthy controls after activation, while the level of total p38 remained unchanged (figure 5A). We also observed a remarkably increased level of ROS in CRP-treated CD8$^+$ T cells (figure 5B), as well as oxidized glutathione (GSSG) (figure 5C). Additionally, in the presence of antibody against CD32b, the activation of p38 MAPK was attenuated (figure 5D). Blockage of CD32b before CRP treatment also inhibited CRP-induced ROS (figure 5E, online supplemental figure S5) and GSSG production (figure 5F). Furthermore, CD32b blockage partially reversed CRP-mediated inhibitory effects of CRP on proliferation (figure 5G) and cytokine production (figure 5H) in CD8$^+$ T cells. Collectively, these results proposed an important role of CRP in regulating CD8$^+$ T cell via p38MAPK/ROS axis in a CD32b-dependent manner.

p38 blockade improves T-cell fitness via ROS and redox metabolic program

p38MAPK-specific inhibitors (p38i) SB202190 indeed inhibited CRP-induced ROS and GSSG production (figure 6A,B). Furthermore, p38i partially abrogated

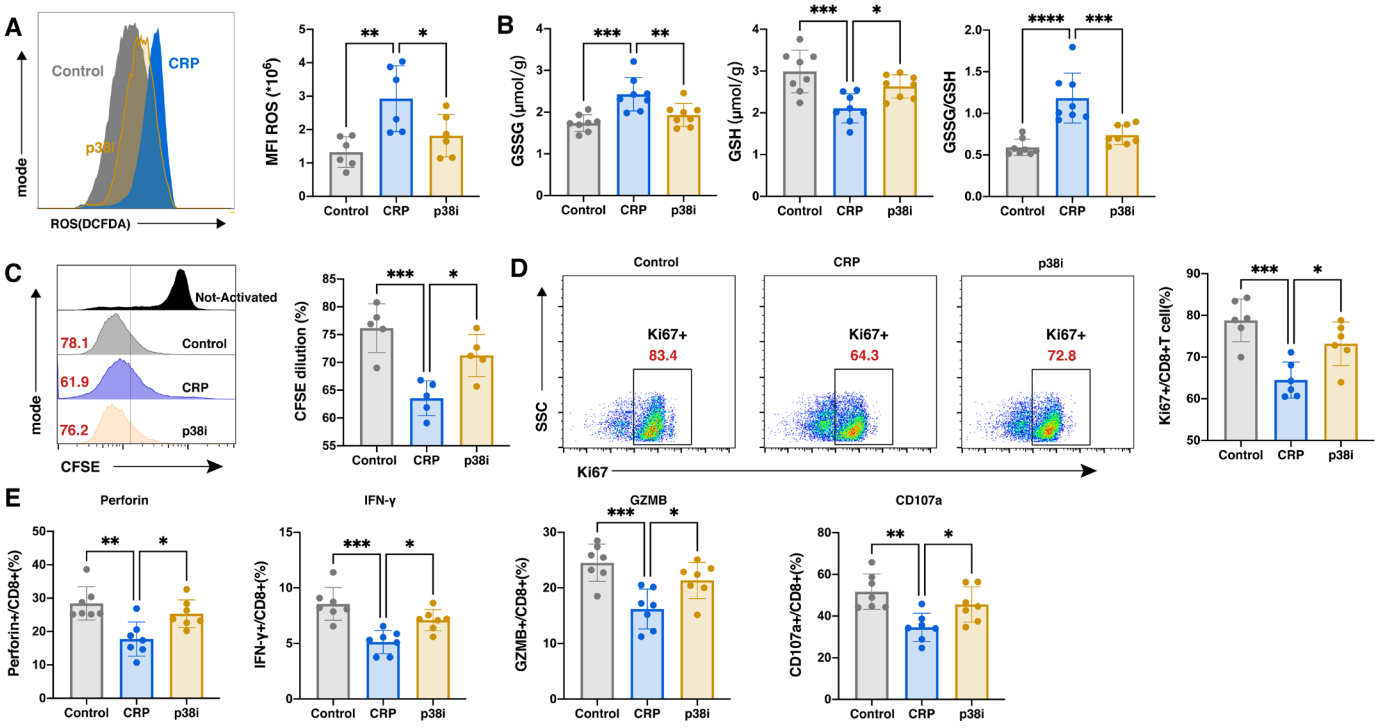

Figure 6 p38 blockade improves T cell fitness via ROS and redox metabolic program. (A) Detection of total cellular ROS in purified CD8$^+$ T cells in the presence CRP with p38i pre-treatment. (B) Quantification of oxidized glutathione and reduced glutathione in CD8$^+$ T cells treated with p38i. (C) Proliferation analysis of Cell Trace CFSE-labeled CD8$^+$ T cells in the presence of p38i. (D) CD8$^+$ T cells with p38i exposure were stained with antibody against Ki67 to detect the proliferation by flow cytometry. (E) The perforin$^+$, GZMB$^+$, IFN-γ$^+$ and CD107a$^+$ T cells proportions (gated on CD8$^+$ T cell) were examined by flow cytometry. Data from eight independent experiments are shown. *p<0.05, p<0.01, ***p<0.001, ****p<0.0001. CRP, C-reactive protein; DCFDA, 2',7'-dichlorofluorescein diacetate; GSH, glutathione; GSSG, oxidized glutathione; GZMB, granzyme B; IFN, interferon; ROS, reactive oxygen species.

the inhibitory effects of CRP on proliferation in CD8$^+$ T cells via CFSE analysis (figure 6C) and Ki67 detection (figure 6D). Similarly, p38i also reversed CRP-mediated downregulation of cytokine production (perforin, GZMB, IFN-γ, CD107a) in CD8$^+$T cells (figure 6E). Altogether, these results indicated that CRP inhibited the function of CD8$^+$ T cells via p38 MAPK pathway.

The inhibitory role of CRP on T cells in MM condition

MM-CTLs were expanded ex vivo with tumor lysate-pulsed DCs acting as autologous APCs in HLA-A*0201 samples exhibited higher activation markers compared with T cells cultured alone without DCs (online supplemental figure S6A,B). CRP exposure in vitro suppressed expansion of MM-CTLs in a dose-dependent manner via detection of Ki67 expression (figure 7A). Based on the CFSE/PI double staining, we observed impaired cytotoxic function in MM-CTL with CRP treatment in a dose-dependent manner (figure 7B, p<0.05), and cytokine production analysis revealed downregulated perforin, GZMB, IFN-γ and CD107a in MM-CTLs treated with CRP (figure 7C), and senescence and exhaustion markers KLRG1, CD57 and LAG3 were upregulated (online supplemental figure S6C,D).

CRP also inhibited BCMA CAR-T cell proliferation (figure 7D) and cytotoxic cytokine secretion, including perforin, GZMB, IFN-γ and CD107a (figure 7F). Decline of cytotoxicity in CAR-T cells with CRP treatment was also shown in figure 7E (p<0.05). CRP incubation also upregulated the expression of KLRG1, CD57 and LAG3 in BCMA CAR-T cells (online supplemental figure S7A,B).

CRP injection resulted in T-cell dysfunction in Vk*MYC myeloma mouse models. First, the percentage of plasma cells were indeed increased in Vk*MYC mice (online supplemental figure S7C). After CRP injection, the infiltration of CD8$^+$ T cells was decreased (online supplemental figure S7D). CD8$^+$ T cells from the BM and spleen both exhibited declined Ki67 expression (figure 7G, p<0.05) and decreased levels of perforin, GZMB, IFN-γ and CD107a with CRP intervention (figure 7H), as well as upregulation of KLRG1 and LAG3 (online supplemental figure S7E,F). Altogether, these results indicated that CRP had an inhibitory impact on T cells in MM condition.

DISCUSSION

CRP levels are found to be remarkably elevated in patients with MM, and previous studies have confirmed the role of CRP in promoting MM cell proliferation and bone destruction.[11 16] However, its direct role in T lymphocytes in MM has not been well elucidated. CRP has been reported to modulate the Th1 and Th2 response and inhibit proliferation, activation associated phenotypes

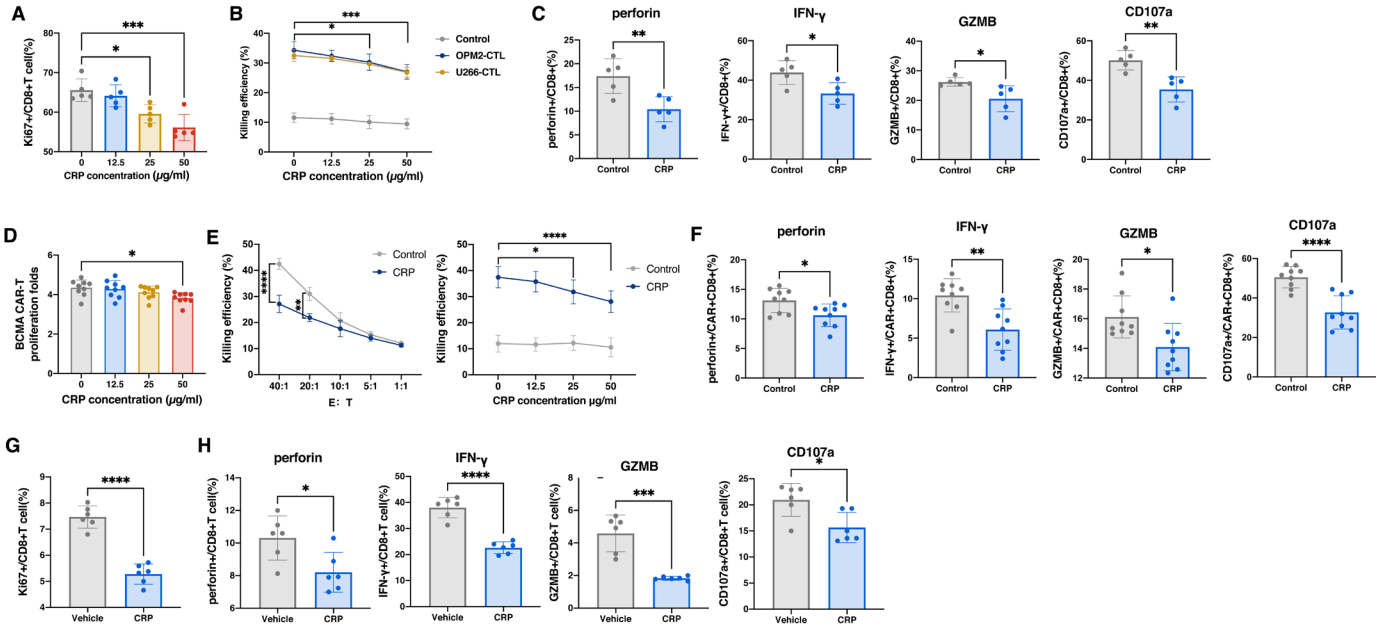

Figure 7 The inhibitory role of CRP on T cells in MM condition. (A) Ki67 expression decreased with treatment of CRP in MM-CTLs in a dose-dependent manner. (B) Cytotoxicity was assessed based on the double positive PI/CFSE population. Lysis of OPM2 or U226 MM cells by MM-CTLs, which were treated with different dose of CRP at E:T=20:1 for 5 days, was analyzed by flow cytometry. (C) The perforin$^+$, GZMB$^+$, IFN-γ$^+$ and CD107a$^+$ T cell proportions (gated on CD8$^+$T cell) were decreased in CRP-treated MM-CTLs. Data from five independent experiments are shown. (D) After treatment of CRP in BCMA CAR-T cells, cell counting results indicated CRP inhibited CAR T-cell proliferation. (E) The CFSE-positive RPMI-8226 cells were gated as target cells, whereas PI-positive cells represented dead cells, and CFSE/PI double-positive cells were calculated as killed target cells. Lysis of RPMI-8226 cells by BCMA CAR-T cells was analyzed by flow cytometry. (F) The perforin$^+$, GZMB$^+$, IFN-γ$^+$ and CD107a$^+$ T cells proportions (gated on CD8$^+$T cell) were decreased in CRP-treated CAR-T cells. Data from nine independent experiments are shown. (G) Proliferation analysis of Ki67$^+$ CD8$^+$ T cells from BM of Vk*MYC mice. (H) The perforin$^+$, GZMB$^+$, IFN-γ$^+$ and CD107a$^+$ T cells proportions (gated on CD8$^+$T cell) from BM of Vk*MYC mice were examined by flow cytometry. Data from six independent experiments are shown. *p<0.05, **p<0.01, ***p<0.001, ****p<0.0001. BCMA, B-cell maturation antigen; BM, bone marrow; CAR, chimeric antigen receptor; CRP, C-reactive protein; GZMB, granzyme B; IFN, interferon; MM, multiple myeloma; MM-CTL, MM-specific cytotoxic T cells.

and the effector function of activated CD4$^+$ and CD8$^+$ T cells in patients with melanoma.[9 10] However, the impacts of CRP on T cells remain elusive in MM. For the first time, our study found that elevated CRP levels were associated with T-cell dysfunction in MM. In the current work, we found CRP induced T-cell senescence, inhibited proliferation and cytotoxic activity in CD8$^+$ T cells from healthy donors, MM-CTL and BCMA CAR-T cells, indicating the inhibitory role of CRP in regulating T-cell function. In our study, results showed the tumor-killing activity of BCMA CAR-T cells was impaired with the increasing concentration of CRP. The result suggested that the therapeutic effect of BCMA CAR-T cell treatment was limited in patients with MM with high CRP levels, which needed more support from clinical data. However, inspired by this, the serum CRP levels of patients with MM may help to choose the best time point for BCMA CAR-T cell treatment.

We found CRP bound to FcγRIIb on T cells, ultimately restricting T-cell function. Previous studies have indicated that CRP could bind to multiple isoforms of FcγRs,[22] which play a pivotal role in immunity, controlling innate and humoral immunity by actuating the effector functions of antibodies.[23] We examined the expression of different FcγR and found only FcγRIIb was expressed on T cells. FcγRIIb is the sole inhibitory Fcγ receptor and well known to be expressed on B cells, macrophages, DCs, and granulocytes.[24] For decades, it has been generally accepted that T cells do not express FcγRIIb.[25 26] Nonetheless, recent study has identified a distinct subset of CD44^{hi} CD8$^+$ T cells that expressed FcγRIIb in both mice and human being.[27] Studies have revealed that the FcγRIIb is upregulated on tumor-infiltrating effector CD8$^+$ T cells in an experimental melanoma model and CD8$^+$ T cells in patients with melanoma. Deficiency of FcγRIIb leads to enhanced tumor-infiltrating T cells and significantly reduced tumor burden.[28] In our study, we demonstrated that the expression of FcγRIIb on CD8$^+$ T cells was significantly increased after activation that allowed CRP to bind to T cells. The expression of CD32b was also increased on T cells from Vk*MYC mice which are challenged by myeloma cells in vivo. Consequently, in our study, we mainly focused on investigating the impact of CRP on activated T cells. However, the mechanisms upregulating the expression of CD32b in T cells remain elusive. Among different subsets in CD8$^+$ T cells, naïve T subset contained the highest frequencies of CD32b$^+$

cells and was the major contributor to bind CRP, which is consistent with previous research that CRP bound to mouse naïve CD4$^+$ T cells.[9] Treatment with CRP for 5 days also decreased the percentage of naïve CD8$^+$ T subset. According to the above results, we speculated that CRP regulated the proliferation and differentiation of naïve T cells after binding to T cells.

We also revealed that CRP inhibited the function of T cells via activating p38 MAPK pathway. There are four isoforms of p38 MAPK including α, β, γ, δ,[29] which can be activated by a wide range of cellular stresses such as ROS[30] as well as inflammatory cytokines.[31] The p38 MAPK pathway is one of the major pathways triggered by TCR,[32] indicating the potential role of p38 MAPK in T-cell activation. In the previous study, inhibition of p38 MAPK promoted T-cell proliferation and expression of CD62L which is a stem cell-like memory marker after activation.[33] The addition of p38 inhibitor, doramapimod or SB202190, to IL-7 and IL-15 culture medium also largely increased the capacity of T cells in the proliferation with enrichment of the naïve-like subsets and expression of CD62L.[32] Inhibiting p38 MAPK pharmacologically improved the effectiveness of murine antitumor T cells and enhanced the function of gene-engineered, tumor-specific T cells in mice.[33] The inhibition of p38 MAPK also augments the T-cell stimulatory capacity of human monocyte-derived DCs in the presence of Treg.[34] Moreover, the p38 MAPK pathway is implicated in T-cell senescence.[35] Research reported that senescent human T cells spontaneously engaged the metabolic master regulator AMPK to trigger recruitment of p38 to the scaffold protein TAB1, which caused autophosphorylation of p38.[36] In our study, we chose the most commonly used p38 inhibitors: SB202190, which is an effective p38 inhibitor and targeting the p38 α and p38 β MAPKs.[37] Our results also indicated p38 MAPK blockade improves T-cell fitness via ROS and redox metabolic program after T-cell activation.

The regulation of ROS and p38 MAPK are interconnected with each other, both being key regulators in inflammatory processes.[38 39] The p38 MAPK pathway is one of the downstream cascades in the ROS signaling pathway which is associated with cell proliferation, differentiation, and apoptosis. Previous researches have also demonstrated that ROS can induce or mediate the activation of p38 MAPK.[33 40–42] However, T cells treated with p38i display decreased intracellular ROS levels as well as mitochondrial ROS levels.[33] DDIT4 coordinates the assembly of the p38-MAPK signaling complex to drive ROS production in an S-nitrosylation dependent manner in liver injury.[40] Collectively, there is a reciprocal regulation between ROS levels and p38 MAPK pathway.

Here we found that CRP induced T-cell senescence, inhibited proliferation and cytotoxic activity in T cells from healthy donors, BCMA CAR-T and MM-specific CTL in vitro and in vivo. Mechanistic studies indicated that CRP bound to surface CD32b/FcγRIIb on activated CD8$^+$ T cells, regulated p38MAPK-ROS pathway and ultimately hampered T cell's proliferation potential and cytotoxicity. These findings contributed to elucidate the mechanisms of CRP inhibiting anti-MM immune response by directly regulating T lymphocytes and provided new insights into T-cell dysfunction in MM.

Correction notice This article has been updated since it was first published online. Jingya Wang has now been listed as a corresponding author.

Acknowledgements We are indebted to all the donors who participated in this study. We are grateful to Dr Wenwen Liu and Dr Li Wang from Department of Geriatrics, Dr Dawei Li from Department of Urology in Renji Hospital for their support of this study. We also thank Dr Lei Yu in Shanghai Unicar-Therapy Bio-medicine Technology for his help in the production of CAR-T cells.

Contributors JH, Jingya Wang and ZL designed the study. JJ and YW obtained blood samples. JJ, ZP and Junying Wang conducted the experiments. JJ and Jingya Wang preformed statistical analyses. JJ, Jingya Wang and MC interpreted the data for the work. All the authors revised the manuscript. JH supervised this work. JH is responsible for the overall content of the paper as guarantor. All authors reviewed and approved the manuscript.

Funding This work was supported by the National Natural Science Foundation of China (81974006), the Shanghai Shenkang Hospital Development Center Funding (SHDC2020CR2070B), and the Interdisciplinary Program of Shanghai Jiao Tong University (ZH2018ZDB02).

Competing interests None declared.

Patient consent for publication Not applicable.

Ethics approval This study involves human participants and was approved by the Ethics Committee of Renji Hospital (approval RA-2019-151). Participants gave informed consent to participate in the study before taking part. Animal studies were approved by the Committee on Animal Research and Ethics of Tianjin Medical University, and all protocols conformed to the Guidelines for Ethical Conduct in the Care and Use of Non-human Animals in Research (TMUaMEC2020016).

Provenance and peer review Not commissioned; externally peer reviewed.

Data availability statement Data are available in a public, open access repository.

ORCID iDs
Jinxing Jiang http://orcid.org/0000-0002-2109-4822
Zhiqiang Liu http://orcid.org/0000-0002-0677-8097

REFERENCES

1 Lu J, Mold C, Du Clos TW, *et al*. Pentraxins and FC receptor-mediated immune responses. *Front Immunol* 2018;9:2607.
2 Hart PC, Rajab IM, Alebraheem M, *et al*. C-reactive protein and cancer-diagnostic and therapeutic insights. *Front Immunol* 2020;11:595835.
3 Lu J, Marjon KD, Mold C, *et al*. Pentraxins and FC receptors. *Immunol Rev* 2012;250:230–8.
4 Roghanian A, Stopforth RJ, Dahal LN, *et al*. New revelations from an old receptor: Immunoregulatory functions of the inhibitory FC gamma receptor, FcγRIIB (CD32B). *J Leukoc Biol* 2018.
5 Enocsson H, Karlsson J, Li H-Y, *et al*. The complex role of C-reactive protein in systemic lupus erythematosus. *J Clin Med* 2021;10:5837.

6 Jimenez RV, Wright TT, Jones NR, *et al*. C-reactive protein impairs dendritic cell development, maturation, and function: implications for peripheral tolerance. *Front Immunol* 2018;9:372.
7 Zhang R, Becnel L, Li M, *et al*. C-reactive protein impairs human CD14+ monocyte-derived dendritic cell differentiation, maturation and function. *Eur J Immunol* 2006;36:2993–3006.
8 Stancel N, Chen C-C, Ke L-Y, *et al*. Interplay between CRP, Atherogenic LDL, and LOX-1 and its potential role in the pathogenesis of atherosclerosis. *Clin Chem* 2016;62:320–7.
9 Zhang L, Liu S-H, Wright TT, *et al*. C-reactive protein directly suppresses Th1 cell differentiation and alleviates experimental autoimmune encephalomyelitis. *J Immunol* 2015;194:5243–52.
10 Yoshida T, Ichikawa J, Giuroiu I, *et al*. C reactive protein impairs adaptive immunity in immune cells of patients with melanoma. *J Immunother Cancer* 2020;8:e000234.
11 Yang J, Wezeman M, Zhang X, *et al*. Human C-reactive protein binds activating Fcgamma receptors and protects myeloma tumor cells from apoptosis. *Cancer Cell* 2007;12:252–65.
12 Chakraborty R, Muchtar E, Kumar SK, *et al*. Elevated pre-transplant C-reactive protein identifies a high-risk subgroup in multiple myeloma patients undergoing delayed autologous stem cell transplantation. *Bone Marrow Transplant* 2018;53:155–61.
13 Heppt MV, Heinzerling L, Kähler KC, *et al*. Prognostic factors and outcomes in metastatic uveal melanoma treated with programmed cell death-1 or combined PD-1/cytotoxic T-lymphocyte antigen-4 inhibition. *Eur J Cancer* 2017;82:56–65.
14 Kim E-S, Kim SY, Koh M, *et al*. C-reactive protein binds to integrin A2 and Fcγ receptor I, leading to breast cell adhesion and breast cancer progression. *Oncogene* 2018;37:28–38.
15 Dupire S, Wemeau M, Debarri H, *et al*. Prognostic value of Pini index in patients with multiple myeloma. *Eur J Haematol* 2012;88:306–13.
16 Yang J, Liu Z, Liu H, *et al*. C-reactive protein promotes bone destruction in human myeloma through the CD32-P38 MAPK-twist axis. *Sci Signal* 2017;10:eaan6282.
17 Yu B, Jiang T, Liu D. BCMA-targeted immunotherapy for multiple myeloma. *J Hematol Oncol* 2020;13:125.
18 Shi X, Yan L, Shang J, *et al*. Anti-CD19 and anti-BCMA car T cell therapy followed by lenalidomide maintenance after autologous stem-cell transplantation for high-risk newly diagnosed multiple myeloma. *Am J Hematol* 2022;97:537–47.
19 Shi L, Campbell G, Jones WD, *et al*. The microarray quality control (MAQC)-II study of common practices for the development and validation of microarray-based predictive models. *Nat Biotechnol* 2010;28:827–38.
20 Chen M, Wan Y, Li X, *et al*. Dynamic single-cell RNA-Seq analysis reveals distinct tumor program associated with microenvironmental remodeling and drug sensitivity in multiple myeloma. *Cell Biosci* 2023;13:19.
21 Jiang J, Xiang J, Chen M, *et al*. Distinct mechanisms of dysfunctional antigen-presenting DCs and monocytes by single-cell sequencing in multiple myeloma. *Cancer Sci* 2023;114:2750–60.
22 Salazar J, Martínez MS, Chávez-Castillo M, *et al*. C-reactive protein: an in-depth look into structure, function, and regulation. *Int Sch Res Notices* 2014;2014:653045.
23 Bournazos S, Ravetch JV. Fcγ receptor function and the design of vaccination strategies. *Immunity* 2017;47:224–33.
24 Bournazos S, Gupta A, Ravetch JV. The role of IgG FC receptors in antibody-dependent enhancement. *Nat Rev Immunol* 2020;20:633–43.
25 Smith KGC, Clatworthy MR. Fcgammariib in autoimmunity and infection: evolutionary and therapeutic implications. *Nat Rev Immunol* 2010;10:328–43.
26 Starbeck-Miller GR, Badovinac VP, Barber DL, *et al*. Cutting edge: expression of FcγRIIB tempers memory CD8 T cell function in vivo. *J Immunol* 2014;192:35–9.
27 Morris AB, Farley CR, Pinelli DF, *et al*. Signaling through the inhibitory FC receptor FcγRIIB induces $CD8^+$ T cell apoptosis to limit T cell immunity. *Immunity* 2020;52:136–50.
28 Farley CR, Morris AB, Tariq M, *et al*. FcγRIIB is a T cell checkpoint in antitumor immunity. *JCI Insight* 2021;6:e135623.
29 Burton JC, Antoniades W, Okalova J, *et al*. Atypical P38 signaling, activation, and implications for disease. *Int J Mol Sci* 2021;22:4183.
30 Nakamura T, Naguro I, Ichijo H. Iron homeostasis and iron-regulated ROS in cell death, senescence and human diseases. *Biochim Biophys Acta Gen Subj* 2019;1863:1398–409.
31 Cuenda A, Rousseau S. P38 MAP-Kinases pathway regulation, function and role in human diseases. *Biochim Biophys Acta* 2007;1773:1358–75.
32 Chen S, Zhang J, Shen M, *et al*. P38 inhibition enhances TCR-T cell function and antagonizes the immunosuppressive activity of TGF-B. *Int Immunopharmacol* 2021;98:107848.
33 Gurusamy D, Henning AN, Yamamoto TN, *et al*. Multi-phenotype CRISPR-Cas9 screen identifies p38 kinase as a target for adoptive immunotherapies. *Cancer Cell* 2020;37:818–33.
34 Lu Y, Zhang M, Wang S, *et al*. P38 MAPK-inhibited dendritic cells induce superior antitumour immune responses and overcome regulatory T-cell-mediated immunosuppression. *Nat Commun* 2014;5:4229.
35 Mathiasen SL, Gall-Mas L, Pateras IS, *et al*. Bacterial genotoxins induce T cell senescence. *Cell Rep* 2021;35:109220.
36 Lanna A, Henson SM, Escors D, *et al*. The kinase P38 activated by the metabolic regulator AMPK and scaffold TAB1 drives the senescence of human T cells. *Nat Immunol* 2014;15:965–72.
37 Bain J, Plater L, Elliott M, *et al*. The selectivity of protein kinase inhibitors: a further update. *Biochem J* 2007;408:297–315.
38 Liu J, Wei Y, Jia W, *et al*. Chenodeoxycholic acid suppresses AML progression through promoting lipid peroxidation via ROS/P38 MAPK/DGAT1 pathway and inhibiting M2 macrophage polarization. *Redox Biol* 2023;59:102566.
39 Yao Y, Cui L, Ye J, *et al*. Dioscin facilitates ROS-induced apoptosis via the P38-MAPK/HSP27-mediated pathways in lung squamous cell carcinoma. *Int J Biol Sci* 2020;16:2883–94.
40 Li Z, Zhao Q, Lu Y, *et al*. DDIT4 s-Nitrosylation AIDS P38-MAPK signaling complex assembly to promote hepatic reactive oxygen species production. *Adv Sci (Weinh)* 2021;8:2101957.
41 Yu Q, Du F, Douglas JT, *et al*. Mitochondrial dysfunction triggers synaptic deficits via activation of P38 map kinase signaling in differentiated alzheimer's disease trans-mitochondrial cybrid cells. *J Alzheimers Dis* 2017;59:223–39.
42 Jha SK, Jha NK, Kar R, *et al*. P38 MAPK and Pi3K/AKT signalling cascades Inparkinson's disease. *Int J Mol Cell Med* 2015;4:67–86.